

Highly efficient red electrophosphorescent devices based on an iridium complex with trifluoromethyl-substituted pyrimidine ligand

Yu-Hua Niu, Baoquan Chen, Sen Liu, Hinlap Yip, Julie Bardecker, Alex K.-Y Jen, Jakka Kavitha, Yun Chi, Ching-Fong Shu, Ya-Hsien Tseng, and Chen-Han Chien

Citation: *Applied Physics Letters* **85**, 1619 (2004); doi: 10.1063/1.1786369

View online: <http://dx.doi.org/10.1063/1.1786369>

View Table of Contents: <http://scitation.aip.org/content/aip/journal/apl/85/9?ver=pdfcov>

Published by the [AIP Publishing](#)

Articles you may be interested in

[Correlation of photoluminescent quantum efficiency and device characteristics for the soluble electrophosphorescent light emitter with interfacial layers](#)

J. Appl. Phys. **104**, 024511 (2008); 10.1063/1.2959817

[White polymeric light-emitting diode based on a fluorene polymer/Ir complex blend system](#)

Appl. Phys. Lett. **86**, 121101 (2005); 10.1063/1.1873046

[Increased electrophosphorescent efficiency in organic light emitting diodes by using an exciton-collecting structure](#)

J. Appl. Phys. **97**, 044505 (2005); 10.1063/1.1853500

[Red electrophosphorescence devices based on rhenium complexes](#)

Appl. Phys. Lett. **83**, 365 (2003); 10.1063/1.1592633

[Highly efficient electrophosphorescent devices based on conjugated polymers doped with iridium complexes](#)

Appl. Phys. Lett. **80**, 2045 (2002); 10.1063/1.1461418

The advertisement features a dark blue background with white and orange text. At the top left, it reads 'NEW! Asylum Research MFP-3D Infinity™ AFM' in large white letters, followed by 'Unmatched Performance, Versatility and Support' in orange. On the right, the Oxford Instruments logo is shown with the tagline 'The Business of Science®'. Below the text are four images: a blue textured surface, a brown textured surface, a grid of colorful squares, and the MFP-3D Infinity AFM instrument itself. Text descriptions are placed around these images: 'Stunning high performance' next to the blue surface, 'Simpler than ever to GetStarted™' next to the brown surface, 'Comprehensive tools for nanomechanics' next to the grid, and 'Widest range of accessories for materials science and bioscience' next to the instrument.

Highly efficient red electrophosphorescent devices based on an iridium complex with trifluoromethyl-substituted pyrimidine ligand

Yu-Hua Niu, Baoquan Chen, Sen Liu, Hinlap Yip, Julie Bardecker, and Alex K.-Y Jen^{a)}
Department of Materials Science and Engineering, Box 352120, University of Washington, Seattle, Washington 98195-2120

Jakka Kavitha and Yun Chi
Department of Chemistry, National Tsing Hua University, Hsinchu 300, Taiwan

Ching-Fong Shu, Ya-Hsien Tseng, and Chen-Han Chien
Department of Applied Chemistry, National Chiao Tung University, Hsinchu 30035, Taiwan

(Received 20 April 2004; accepted 22 June 2004)

Highly efficient red-emitting electrophosphorescent devices were fabricated by doping an iridium (Ir) complex containing trifluoromethyl (CF₃)-substituted pyrimidine ligand into a conjugated bipolar polyfluorene with triphenylamine and oxadiazole as side chains. The device efficiency can be enhanced through effective exciton confinement using a layer of 1,3,5-tris(*N*-phenylbenzimidazol-2-yl)benzene on the cathode side and a layer of *in situ* polymerized tetraphenyldiamine-perfluorocyclobutane on the anode side. For a blend with 5 wt % of the Ir complex, a maximum external quantum efficiency of 7.9 photon/electron % and a maximum brightness of 15800 cd/m² are reached with Commission Internationale de L'Eclairage chromaticity coordinates of $x=0.65$ and $y=0.34$. © 2004 American Institute of Physics. [DOI: 10.1063/1.1786369]

Organic and polymer light-emitting diodes (LEDs) based on fluorescent molecules or polymers have attracted great interest because of their potential for applications in flat-panel displays. However, the probability of singlet exciton formation in the charge recombination process of fluorescent LEDs is only 25% by simple spin-pairing statistics. Thus, the highest efficiency achievable of these devices is quite limited. Fortunately, this upper limit can be overcome by using phosphorescent complexes as dopants in LEDs to harvest both singlet and triplet excitons. This phenomenon increases the internal quantum efficiency to that of almost 100%.^{1,2}

The iridium complexes developed by Thompson *et al.*³ containing the 2-phenyl pyridine type cyclometalated ligands, such as Ir(ppy)₃, have been extensively studied for the fabrication of green LEDs.³ The strong emission occurring at $\lambda_{\max}=514$ nm is believed to originate from the triplet manifold containing both the intraligand $\pi-\pi^*$ and the metal-to-ligand charge transfer (MLCT) characters. It is anticipated that color tuning from green to red can be achieved by lowering the energy gap of either the $\pi-\pi^*$ or the MLCT excited states. To test this hypothesis, we replace the pyridine by a pyrimidine fragment, which contains two electronegative nitrogen atoms on the aromatic π -skeleton, and incorporate an additional electron-withdrawing CF₃ group. As a result, a red-emitting iridium complex with two CF₃-substituted pyrimidine ligands, (napm)₂Ir(bppz)CF₃ (Ir-1, Fig. 1), was synthesized.⁴ In solid state, when excited, the Ir-1 exhibits a pure red emission peak at 638 nm, as shown in Fig. 2. From the featureless broad emission, it can be judged as the characteristic of triplet metal-to-ligand charge-transfer (³MLCT).⁵

To use this complex as the electroluminescent (EL) layer in LEDs, it is crucial to blend the triplet emitter into a suit-

able host. In general, there are two possible mechanisms involved in this process: The Förster/Dexter energy transfer or the direct charge-trapping and recombination mechanism. In the former process, excitons that are formed in the host migrate to the triplet dopant via the dipole resonance coupling or charge exchange.^{6,7} In the latter process, charge carriers are directly trapped by the guest and await the arrival of opposite carriers for recombination.⁸ In either case, a host

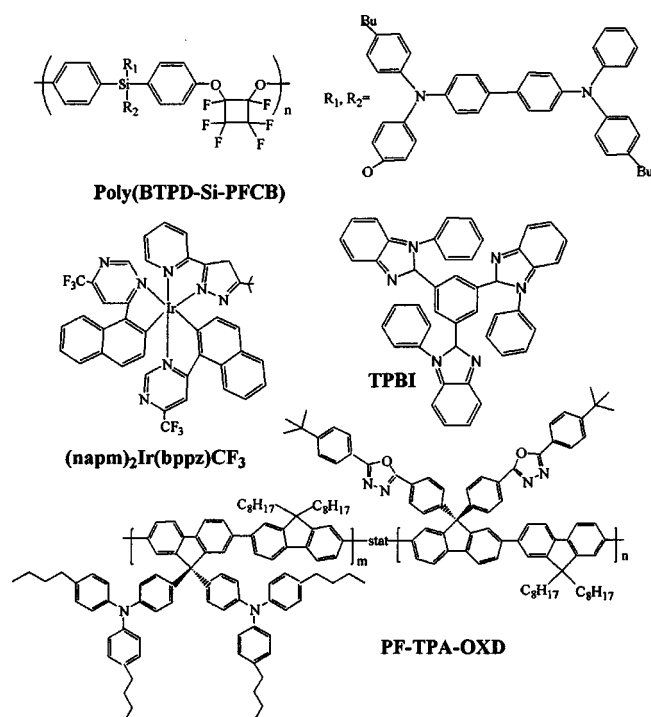


FIG. 1. Chemical structures of the cross-linked hole-transport material, poly(BTPD-Si-PFCB), the electron-transport material, TPBI, and the host polymer, PF-TPA-OXD.

^{a)}Electronic mail: ajen@u.washington.edu

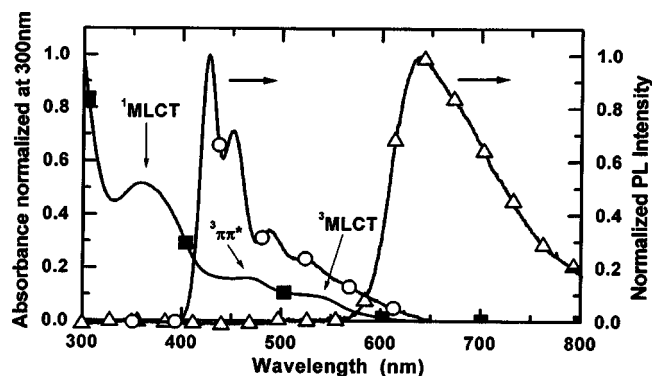


FIG. 2. UV-VIS absorbance spectrum (■) and PL spectrum (△) of the Ir-complex and PL spectrum of the host, PF-TPA-OXD (○).

with balanced electron and hole transport abilities should be beneficial. Therefore, a bipolar blue-emitting polyfluorene with hole-transporting triphenylamine (TPA) and electron-transporting oxadiazole (OXD) as side chains (PF-TPA-OXD, Fig. 1) was chosen as host.⁹

To realize high efficiency, hole blocking at the cathode side and electron-blocking at the anode side as well as effective exciton confinements are necessary. In this letter, we adopt a tetraphenyldiamine-based hole-injection/transport layer (HTL), poly(BTPD-Si-PFCB) (HP1, Fig. 1),¹⁰ which functions both as an electron-blocking and an exciton-confinement layer at the anode side. In the meantime, a layer of 1,3,5-tris(*N*-phenylbenzimidazol-2-yl)benzene (TPBI, Fig. 1) electron-injection/transport layer (ETL) was also used at the cathode side for hole blocking and exciton confinement.¹¹ For a blend with 5 wt % of the Ir complex in PF-TPA-OXD, a maximum external quantum efficiency of 7.9 photon/electron (ph/el)% and a maximum brightness of 15 800 cd/m² are reached with Commission Internationale de L'Eclairage (CIE) chromaticity coordinates of $x=0.65$ and $y=0.34$. These results are outstanding for red LEDs using a phosphorescent emitter as dopant in conjugated polymer.

Solution blending of Ir-1 and PF-TPA-OXD was carried out at specific volume ratios using separate solution matrices with a concentration of 10 mg/ml in *p*-xylene. Compared with the process of using multisources cosublimation in organic LEDs the solution blending process can control the ratio precisely. The LEDs were fabricated on indium-tin-oxide (ITO) covered glass substrates. A layer of robust HP1 (~30 nm) with good solvent resistance was prepared by spin coating its precursor (with the concentration of 10 mg/ml in dichloroethane) onto ITO and thermally cross linking it at 225 °C for 40 min under argon. The control devices were prepared by spin coating a layer of polyethylene dioxythiophene polystyrene sulfonate (PEDOT:PSS, Bayer AG) film (~30 nm) on ITO as the HTL. Light-emitting layer (EM) with a nominal thickness of ~40 nm was spin coated on top of HP1, or on the vacuum dried PEDOT:PSS in some cases. TPBI was then sublimed as the ETL (~30 nm) under a vacuum below 1×10^{-6} Torr. Cesium fluoride with thickness of 1 nm and aluminum with thickness of 200 nm were evaporated subsequently as cathode.¹²

The ultraviolet-visible (UV-VIS) absorption spectrum of Ir-1 and the photoluminescence (PL) spectrum of the PF-TPA-OXD are shown in Fig. 2. The absorption peaks of Ir-1 at ~360 nm, ~470 nm and ~540 nm correspond to the singlet metal-to-ligand charge-transfer (¹MLCT) transition,

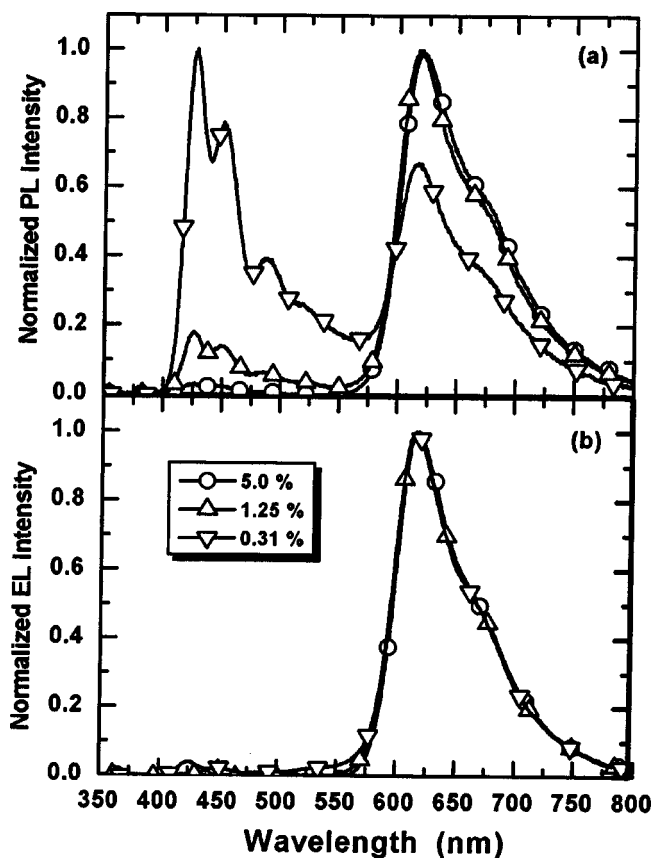


FIG. 3. (a) PL spectra of the spin-coated films of the PF-TPA-OXD:Ir-1 blends with different Ir-1 content. (b) EL spectra from corresponding LEDs with the blends as EL layer.

the ligand-centered $\pi-\pi^*$ transition and the ³MLCT transition, respectively. From the moderate overlap between the PL spectrum of PF-TPA-OXD and the ¹MLCT absorption, it implies that the energy transfer between PF-TPA-OXD and Ir-1 will only be moderate. Consistent with this, Fig. 3(a) shows that for spin-coated films on glass, a blend of more than 5 wt % of Ir-1 in PF-TPA-OXD is necessary to fully quench the emission from the host. However, in a sharp contrast to the PL behavior, the EL spectra [Fig. 3(b)] from LEDs with HP1 as the HTL and TPBI as the ETL show only the guest ³MLCT emission for Ir-1 dopant concentration as low as 0.31 wt %. The dramatic difference between the EL and PL spectra is a very good indication of the dominating role of direct charge trapping and recombination in the EL process. The CIE coordinates from a LED based on the 5 wt % Ir-1 blend are $x=0.65$ and $y=0.34$, very close to the NTSC red standards, $x=0.67$ and $y=0.33$.

Among the blends with an Ir-1 content of 5, 1.25, and 0.31 wt %, the 5 wt % one shows the best device performance. The performance parameters of LEDs based on the 5 wt % blend with different HTL and ETL configurations are listed in Table I for comparison. The device with exciton-confinement layer at both the anode and the cathode side, i.e., the one with structure ITO/HP1/EM/TPBI/CsF/Al, gives the highest performance. Compared to the device that does not use the TPBI as the ETL, the maximum efficiency and brightness are almost doubled. The turn-on voltage is 4.8 V and the maximum external quantum efficiency reaches 7.9 ph/el% at low current density. Even at a high current density of 100 mA/cm², the external quantum efficiency can

TABLE I. Performance of LEDs based on blend of 5 wt % Ir-1 in PF-TPA-OXD with different HTL and ETL configurations.

HTL	PEDOT:PSS		
	HP1	HP1	HP1
ETL	TPBI	TPBI	none
Turn-on voltage (V)	7.8	4.8	4.5
Maximum $\eta_{\text{ext}}(\text{ph/el}\%)$	1.2	7.9	3.6
Maximum brightness (cd/m^2) at driving voltage (V)	1130	15 800	8766
Luminance (cd/m^2) at 10 mA/cm ²	95	480	202
Driving voltage (V) at 10 mA/cm ²	10.3	7.7	6.2
$\eta_{\text{ext}}(\text{ph/e}\%)$ at			
1 mA/cm ²	1.1	5.9	3.2
10 mA/cm ²	0.81	4.2	2.5
100 mA/cm ²	0.51	2.8	1.8
Power efficiency (lm/W) at 1 mA/cm ²	0.54	3.3	1.9

Note: HP1 denotes poly(BTPD-Si-PFCB).

still retain at 2.8 ph/el%. The current density–voltage (J – V) and brightness–voltage (B – V) characteristics shown in Fig. 4 reveal clearly that without TPBI as the hole-blocking/exciton confinement layer, most of the injected holes can penetrate through the device, being wasted without contributing to the light emission. The clear difference of the device performance demonstrates the advantages of confining excitons, as depicted by the energy levels of HP1, PF-TPA-OXD, and TPBI (inset of Fig. 4).

It is interesting to notice that for a device with PEDOT:PSS as the HTL, the performance is very poor. It

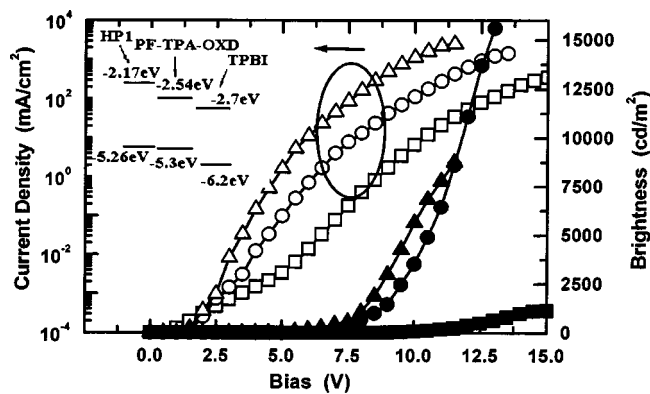


FIG. 4. J – V (open) and B – V (solid) characteristics of the LEDs based on blend of 5% Ir-1 in PF-TPA-OXD. The rectangle corresponds to a LED with structure ITO/PEDOT:PSS/EM/TPBI/CsF/Al, the circle to ITO/HP1/EM/TPBI/CsF/Al, while the triangle to ITO/HP1/EM/CsF/Al. Inset: Energy levels of HP1, PF-TPA-OXD, and TPBI.

may be partially due to the lack of electron-blocking/exciton confinement in these devices. Another possible reason may be due to the serious quenching effect caused by the acidic nature of PEDOT:PSS or the unfavorable phase separation between Ir-1 and PF-TPA-OXD host caused by the hydrophilic characteristic of the lower PEDOT:PSS layer. Detailed investigation on the mechanisms and the effect of different HTLs on the photophysical characteristics of the phosphorescent devices is under way and the results will be published elsewhere.

In conclusion, highly efficient red phosphorescent LEDs are fabricated using an Ir(III)-complex containing two CF₃-substituted pyrimidine ligands in a bipolar polyfluorene. A maximum external quantum efficiency of 7.9 ph/el% and a brightness of 15 800 cd/m^2 are reached with the CIE chromaticity coordinates of $x=0.65$ and $y=0.34$. Efficient and balanced charge injection and transport, as well as effective carrier blocking and exciton confinement, at both electrode sides contribute to the high performance.

This work was supported by the National Science Foundation (NSF-STC Program under Agreement No. DMR-0 120967) and the Air Force Office of Scientific Research (AFOSR) under the MURI Center on Polymeric Smart Skins. One of the authors (Y.C.) thanks the National Science Council of Taiwan, R.O.C. for the financial support (NSC 91-2119-M-002-016) and (NSC 91-2113-M-007-006). Another author (A.K.-Y.J.) thanks Boeing–Johnson Foundation for its support.

- ¹C. Adachi, M. A. Baldo, M. E. Thompson, and S. R. Forrest, *J. Appl. Phys.* **90**, 5048 (2001).
- ²M. Ikai, S. Tokito, Y. Sakamoto, T. Suzuki, and Y. Taga, *Appl. Phys. Lett.* **79**, 156 (2001).
- ³M. A. Baldo, M. B. Thompson, and S. R. Forrest, *Nature (London)* **403**, 750 (2000).
- ⁴J. Kavitha, Y. Chi, Y.-H. Song, S.-L. Wang, Y.-H. Niu, A. K.-Y. Jen, C.-F. Shu, R. Dodda, and F.-I. Wu (unpublished).
- ⁵J. B. Birks, *Photophysics of Aromatic Molecules* (Wiley-Interscience, London, 1970).
- ⁶T. Förster, *Discuss. Faraday Soc.* **27**, 7 (1959).
- ⁷D. L. Dexter, *J. Chem. Phys.* **21**, 836 (1953).
- ⁸X. Gong, J. C. Ostrowski, D. Moses, G. C. Bazan, and A. J. Heeger, *Adv. Funct. Mater.* **13**, 439 (2003).
- ⁹C.-F. Shu, R. Dodda, K.-I. Wu, M. S. Liu, and A. K.-Y. Jen, *Macromolecules* **36**, 6698 (2003).
- ¹⁰X. Jiang, S. Liu, M. S. Liu, P. Herguth, A. K.-Y. Jen, H. Fong, and M. Sarikaya, *Adv. Funct. Mater.* **12**, 745 (2002).
- ¹¹Y. Li, M. K. Fung, Z. Xie, S.-T. Lee, L.-S. Hung, and J. Shi, *Adv. Mater. (Weinheim, Ger.)* **14**, 1317 (2002).
- ¹²T. M. Brown, R. H. Friend, I. S. Millard, D. J. Lacey, J. Burroughes, and F. Cacialli, *Appl. Phys. Lett.* **93**, 6159 (2003).